JOURNAL OF MATERIALS SCIENCE 16 (1981) 853–862

The effect of grinding direction on flaw character and strength of single crystal and polycrystalline ceramics

R. W. RICE, J. J. MECHOLSKY, Jr, P. F. BECHER
Naval Research Laboratory, Washington, D.C. 20375, USA

The effect upon the room-temperature strengths and fractures of flexure bars caused by grinding them either parallel or perpendicular to their tensile axis was investigated for selected single- and polycrystalline ceramics. Particular attention was given to the character of the flaws from which failure initiated. It was shown that grinding introduces two basic sets of flaws: one set forms at an average angle of ~ 0°, and the other at an average angle of ~ 90°, to the grinding direction. The angles of these flaws varied somewhat due to their formation on preferred fracture planes in single-crystal or larger-grain polycrystalline bodies as well as due to statistical effects. However, overall, the difference in these two sets of flaws was a major factor in the effect of grinding direction on strength. Flaws that formed approximately parallel with the grinding direction were typically more severe, and hence lead to lower strengths for grinding perpendicular to the bar axis, i.e. when the stress was perpendicular, or nearly so, to them.

1. Introduction

Machining often plays a dominant role in the strength of ceramic materials. Despite its important role, information concerning the nature of the machining flaws causing failure has almost always been obtained only by indirect means, primarily by fracture mechanics predictions. Very little direct determination of machining flaw character has been conducted to confirm these predictions. Further, the cause of the significant strength anisotropy that results in many ceramic materials from machining parallel or perpendicular to the axis of subsequent stressing to failure [1] has not been generally determined.

Recent fractographic studies of glass have successfully identified the character of machining flaws causing mechanical failure [2]. These studies showed that the predominant cause of strength anistropy as a function of grinding direction was the difference in the character of the machining flaws rather than the directionality of the grinding striations. On the other hand, recent studies of sapphire [3] indicate that grinding striations may be a factor in strength anisotropy from grinding for some orientations. This paper extends grinding studies to polycrystalline ceramic materials and further examines single crystals showing machining phenomena basically similar to those found in glasses.

2. Experimental procedures

The materials investigated were primarily commercial single crystal and commercial or laboratory polycrystalline samples with less than 2%, and usually less than 0.5%, porosity. Most of these materials have been described in previous investigations by the authors [1, 3–5]. The source and character of additional materials are briefly noted in conjunction with the results on them (see Tables I and II). Emphasis was placed on selecting materials with a fracture character that was amenable to clear fracture initiating flaw determination.

Machining parameters were as in previous studies [1–4]: bars, having approximate cross sectional dimensions of 2.54 mm x 5.08 mm and lengths of 20 to 40 mm, were ground with either a 10 cm diameter 325 grit vitreous bonded diamond wheel rotating at 7900 rpm or a 20 cm

0022–2461/81/040853–10$03.00/0

TABLE I Effect of grinding direction of strength of $MgAl_2O_4$ crystals*

Orientation		Number of specimens per test	Modulus of rupture (MPa)	
Tensile surface	Tensile axis		∥†	⊥†
{1 0 0}	⟨1 0 0⟩	4	269 ± 7	200 ± 10
{1 0 0}	⟨1 1 0⟩	5	190 ± 30	150 ± 20
{1 1 0}	⟨1 0 0⟩	4	210 ± 20	165 ± 30
{1 1 0}	⟨1 1 0⟩	5	430 ± 30	275 ± 35
{1 1 0}	⟨1 1 1⟩	4	330 ± 7	270 ± 30
{1 1 1}	⟨1 1 0⟩	7	240 ± 40	200 ± 40

*Czochralski, stoichiometric Crystals from Union Carbide Corp.
†∥ and ⊥ indicate bar ground respectively parallel with and perpendicular to the tensile (bar) axis.

diameter 325 grit metal bonded wheel rotating at 1725 rpm, using a typical water soluble coolant. Up and down grinding was performed, respectively, on alternate passes with a typical down-feed of 0.05 mm per pass and with feed rates of the order of 6–12 mm sec^{-1}.

Grinding was conducted either parallel or perpendicular to the bar length and, hence, to the axis of subsequent strength testing. Results were obtained over a period of several years with several operators and grinding wheels, and hence should be representive of fairly general practice.

The long edges of the machined bars were rounded by hand on 400 and then 600 grit SiC sandpaper (dry) prior to subsequent 3-point flexure testing at room temperature with a 1.25 mm min^{-1} cross-head travel rate. The resultant fracture surfaces were examined by optical and scanning electron microscopy using river or fracture step, mist and hackle patterns to identify fracture origins [6].

3. Results and discussion

3.1. Single crystals

3.1.1. Cubic single crystals

Stoichiometric Czochralski $MgAl_2O_4$ crystals showed strength anisotrophy as a result of grinding both parallel with and perpendicular to the tensile axis in essentially all crystal orientations tested (see Table I). Similar results have been reported earlier for $3MgO \cdot 3.5Al_2O_3$ Verneuil crystals [1]. When the tensile axis was perpendicular to the {1 1 0} and, especially, {1 0 0} planes, fractures were usually perpendicular to the tensile axis. The fractures were quite flat and sufficiently definitive that flaws could be determined for quantative analysis. This analysis showed that flaws causing failure from grinding perpendicular to the tensile axis were more elongated and of greater depth than flaws causing failure from grinding parallel with the tensile axis, see Fig. 1. Thus, as with glasses [2], there are basically two sets of flaws generated: one set of smaller, approximately circular flaws perpendicular to the grinding direction, and another set of larger, more elongated flaws, parallel with the grinding direction. The orthogonality of preferred fracture planes in cubic $MgAl_2O_4$ allows both sets of flaws to form on these planes when grinding is parallel with or perpendicular to a preferred plane.

Though limited, those cases for which a direct comparison was possible showed that the flaw differences were quantitively consistent with the strength anisotropy (see Table II). Also, fracture energies calculated from strengths and flaw measurements (see Fig. 1 caption) agree well with the value of about 2 J m^{-2} measured by double cantilever beam tests.

Other crystal orientations fractured on combinations of {1 0 0}, {1 1 0} or both planes, as also shown previously [6]. Though the more complex character of these fractures made analysis more difficult, failure generally appeared to originate from flaws on {1 0 0} or {1 1 0} planes and the flaws appeared to have similar anisotropy of shape as a function of grinding direction as found for the above flat fractures (Fig. 1). While the general trends were similar to those for glasses, there were some crystallographic effects on flaw shape, see Fig. 4 of [4].

3.1.2. Non-cubic crystals

Both Al_2O_3 and TiO_2 crystals clearly showed strength anisotropy as a result of the grinding direction being parallel with or perpendicular relative to the bar axis. Rutile data is shown in Table II, Verneuil [1] and Czochralski [3] Al_2O_3 crystal data are presented elsewhere. Fracture of these crystals was, of course, more complicated due to the smaller number of preferred fracture planes and the frequent lack of their orthogonality with one another, as discussed below. However, Al_2O_3 and TiO_2 crystals orientated so that a preferred fracture plane (or surface, since non-cleavage, somewhat choncidal fracture was observed) was, at least approximately perpendicular to or parallel with the grinding direction also generally showed trends similar to those found in glasses [2]. Thus Al_2O_3 and TiO_2 exhi-

TABLE IIA Effect of grinding on flaw geometry of single crystal ceramics

Single crystals	Orientation		Grinding direction*	Number of specimens	Fracture stress	Smallest flaw dimension c (μm)	Ratio a/b	Ratio $\sigma_\perp/\sigma_\parallel$	B
	Tensile surface	Tensile axis							
$MgAl_2O_4$	(1 1 0)	$\langle\bar{1}\,0\,0\rangle$	$\parallel$	3	217 ± 28	15 ± 0	0.4 ± 0.6	0.8	0.8
			$\perp$	3	165 ± 28	14 ± 7	0.4 ± 0.6		
TiO_2	(1 1 0)	$\langle\bar{1}\,1\,0\rangle$	$\parallel$	6	113 ± 7	25	0.7	1.1	0.9
			$\perp$	6	120 ± 4	30	0.7		
TiO_2	(0 0 1)	$\langle 1\,\bar{1}\,0\rangle$	$\parallel$	5	113 ± 3	30	1.5	0.7	0.7
			$\perp$	5	77 ± 3	70	1.5		
TiO_2	(1 0 0)	$\langle 0\,1\,0\rangle$	$\parallel$	6	288 ± 19	–	–	0.83	–
			$\perp$	5	239 ± 12	25	1.3		
TiO_2	(0 0 1)	$\langle 0\,1\,0\rangle$	$\parallel$	5	108 ± 6	60	1.3	1.0	0.9
			$\perp$	5	103 ± 6	70	1.3		
TiO_2	(1 0 0)	$\langle 0\,0\,1\rangle$	$\parallel$	8	285 ± 86	10	0.4	0.6	0.5
			$\perp$	7	183 ± 36	35	0.18		

TABLE IIB Effect of grinding on flaw geometry of polycrystalline ceramics

Single crystals	Grain size (μm)	Grinding direction*	Number of specimens	Fracture stress	Smallest flaw dimension c (μm)	Ratio a/b	Ratio $\sigma_\perp/\sigma_\parallel$	B
Keatite glass ceramic	< 1	$\parallel$	6	180 ± 39	16 ± 5	0.9 ± 0.4	0.6	0.5
		$\perp$	7	102 ± 8	36 ± 15	0.5 ± 0.2		
MgF_2	< 1	$\parallel$	10	87 ± 2	54 ± 21	1.1 ± .07	0.6	0.6
		$\perp$	10	53 ± 2	89 ± 20	0.5 ± .08		
Mullite	1–3	$\parallel$	7	319 ± 35	41 ± 23	1.0 ± 0	0.8	1.0
		$\perp$	6	259 ± 54	24 ± 5	0.4 ± 0.3		
B_4C	2–10	$\parallel$	5	374 ± 69	19 ± 3	1.0 ± 0	0.6	0.8
		$\perp$	9	154 ± 24	26 ± 10	0.2 ± 0.07		
B_4C	100–200	$\parallel$	4	282 ± 228	19 ± 9	0.7 ± 0.5	0.9	0.7
		$\perp$	6	250 ± 55	23 ± 3	0.3 ± 0.2		
CaF_2	50–150	$\parallel$	3	50 ± 13	23 ± 7	0.7 ± 0.2	0.8	0.8
		$\perp$	3	40 ± 5	33 ± 7	0.6 ± 0.6		
Yttralox	100–200	$\parallel$	6	99 ± 6	36 ± 13	0.8 ± 0.3	0.8	0.9
		$\perp$	7	77 ± 8	44 ± 20	0.7 ± 0.3		

*Grinding direction relative to tensile axis.
†Smallest flaw dimension is the smallest of a or b (see ‡).
‡b is the flaw half length along surface; a is the flaw depth.
§Ratio of fracture stresses for perpendicular and parallel grinding.
¶ $B = \frac{\Phi_\perp}{\Phi_\parallel}\left(\frac{c_\parallel}{c_\perp}\right)^{1/2}$, where $c_\parallel$ and $c_\perp$ are the smallest flaw dimension for parallel and perpendicular grinding respectively, and $\Phi_\parallel$ and $\Phi_\perp$ are the respective elliptic integrals for the flaw shapes.

bited a clear trend for flaws from perpendicular grinding to extend deeper into the specimen and be more elongated along the tensile surface, in contrast to the more nearly circular flaws from parallel grinding (Figs 2 and 3 and see also Fig. 8 of [7]). Results for TiO_2, which was studied more extensively, clearly showed that the differences in flaw shape quantitively explained the anisotropy of strength (Table II). Though less extensive, especially for direct comparison of specific orientations, data for Al_2O_3 showed that flaw character was a major factor in strength anisotropy for those orientations giving reasonably flat fractures, i.e. those for which the grinding direction was approximately perpendicular for a preferred fracture surface.

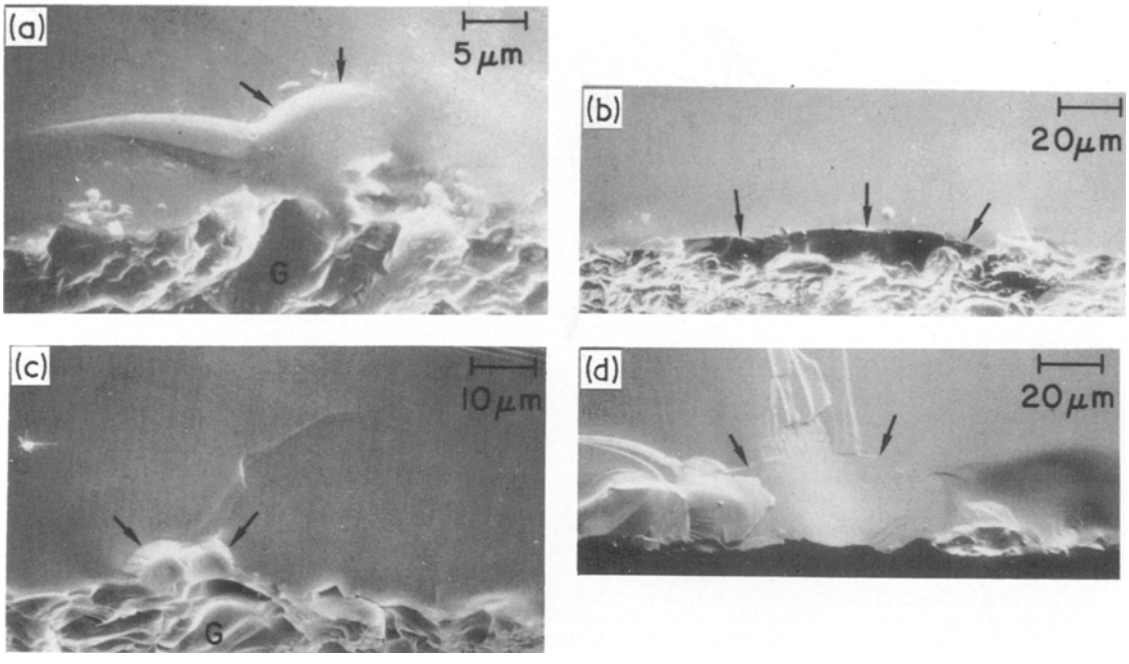

Figure 1 Fracture initiating machining flaws in stoichiometric $MgAl_2O_4$ crystals having $\{1\,1\,0\}$ tensile surfaces. (a) A nearly circular flaw (arrowed) associated with a deep gouge (G) from grinding parallel with the $\langle 1\,0\,0\rangle$ tensile (bar) axis; note the difference in orientation of the flaw and fracture surfaces. (b) An elongated fracture initiating flaw (arrowed) associated with grinding perpendicualr to the $\langle 1\,0\,0\rangle$ tensile (bar) axis. (c) A flaw origin (arrowed), associated with a locally deeper grinding gouge (G) from grinding parallel with the $\langle 1\,1\,1\rangle$ tensile (bar) axis. This is typical of fracture origins on rough $\{1\,0\,0\}$ or $\{1\,1\,0\}$ fracture surface and of flaw variations from such parallel grinding, regardless of crystal orientation. (d) An elongated, more complex flaw (arrowed), representative of flaw variations that can occur from grinding perpendicular to the tensile (bar) axis ($\langle 1\,0\,0\rangle$ in this case). The fracture stresses and resultant calculated fracture energies are: (a) ~ 210 MPa, 1.5 J m^{-2}; (b) ~ 163 MPa, ~ 1.8 J m^{-2}; (c) ~ 325 MPa, ~ 2.5 J m^{-2}; (d) ~ 132 MPa, ~ 1.8 J m^{-2}.

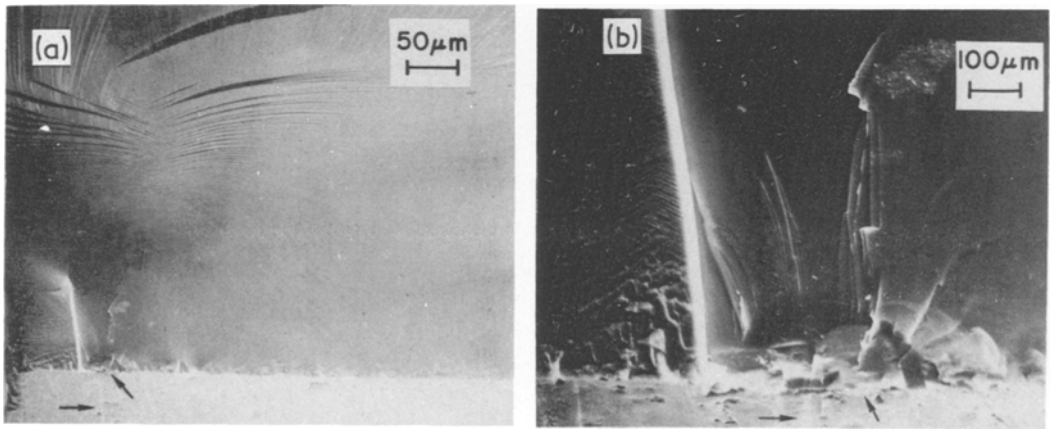

Figure 2 Failure initiation in a TiO_2 crystal ground parallel with the tensile axis. (a) and (b) are lower and higher magnification photographs of much of the fracture and the fracture origin, respectively. Note the failure initiating flaw (arrow at 45° to horizontal) associated with a deeper than average grinding groove (horizontal arrow). The nearly vertical white mark to the left of the fracture origin is a crack approximately parallel with the tensile axis. Failure stress 98 MPa.

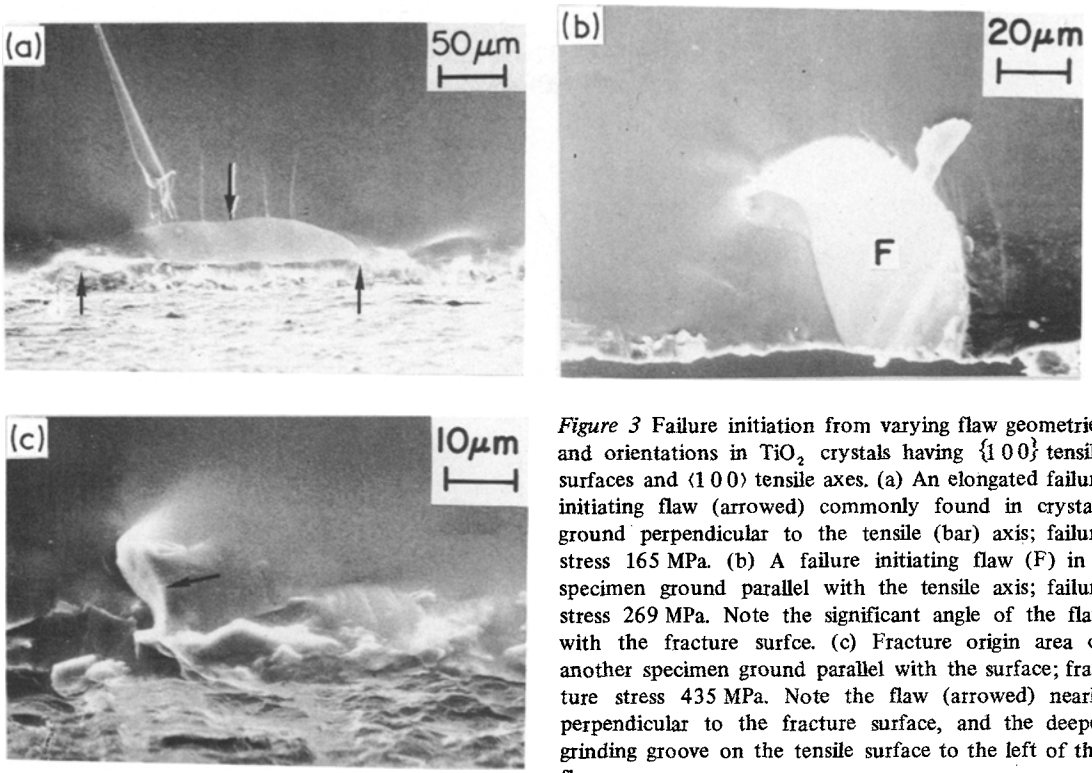

Figure 3 Failure initiation from varying flaw geometries and orientations in TiO_2 crystals having {1 0 0} tensile surfaces and ⟨1 0 0⟩ tensile axes. (a) An elongated failure initiating flaw (arrowed) commonly found in crystals ground perpendicular to the tensile (bar) axis; failure stress 165 MPa. (b) A failure initiating flaw (F) in a specimen ground parallel with the tensile axis; failure stress 269 MPa. Note the significant angle of the flaw with the fracture surfce. (c) Fracture origin area of another specimen ground parallel with the surface; fracture stress 435 MPa. Note the flaw (arrowed) nearly perpendicular to the fracture surface, and the deeper grinding groove on the tensile surface to the left of this flaw.

Flaw and failure variations from those found in glasses, were more common in the non-cubic crystals. Thus, flaws and associated fracture initiation on planes not perpendicular to the stress axis were more frequent, as might have been expected, because of the non-orthogonality of many preferred fracture planes, for example see Fig. 3. Also, cases of fracture initiation from a portion of a flaw parallel with the tensile and grinding axis were more common (but still limited) in non-cubic crystals. Again, this is probably due to greater variation in the orientation of preferred fracture planes.

3.2. Polycrystalline bodies

3.2.1. Fine-grain polycrystalline bodies

Twelve fine-grain polycrystalline bodies having grains of size about 10 microns, and more commonly only a few microns, were studied. All specimens exhibited substantial strength anisotropy as a result of stressing parallel with or perpendicular to the grinding direction (see Table II and see [1] for earlier data). Strengths for stressing perpendicular to the grinding direction were typically nearly 50% less than for stressing parallel with the grinding direction.

Very definitive flaws at fracture origins could be detected in those bodies exhibiting mostly transgranular failure, such as mullite, spinel, β-Al_2O_3 and MgF_2. Flaws were often less definitive in other bodies, primarily those exhibiting a substantial amount of intergranular failure such as Al_2O_3 and Si_3N_4; however, all of these bodies showed the same trend, namely, longer, more severe flaws parallel with the grinding grooves and approximately circular, less severe flaws perpendicular to the grinding grooves, e.g. Figs 4 and 5. Additional examples of definitive machining flaws in fine-grain bodies illustrating these flaw shape differences have been published elsewhere [4, 6, 8]. The size and shape of the machining flaws that Bansal and colleagues identified as fracture origins in a commercial crystallized glass (Pyroceram 9606) [10] and Al_2O_3 [11] are similar in character (e.g. about 20 μm depth) to those the authors have found in these same materials as well as the other polycrystalline materials in this study.

Numerical data on flaw parameters and strength anisotropy is given in Table II for materials in which more extensive direct comparison was obtained. Note that, in general, the fracture energies calculated from the observed flaw sizes

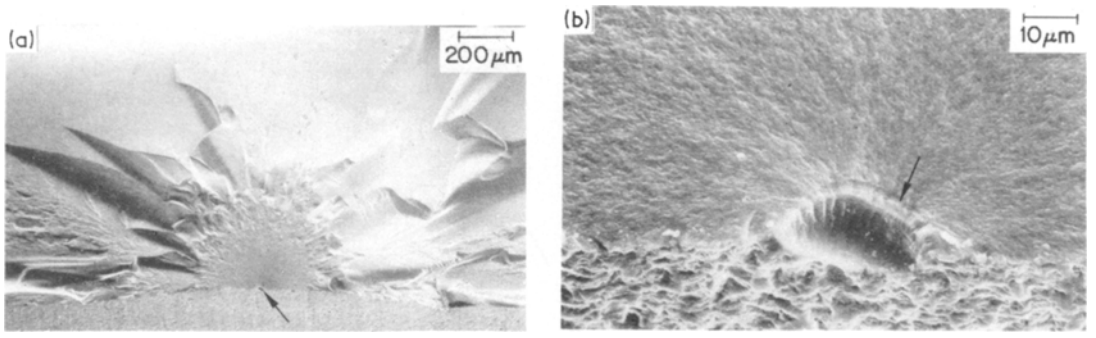

Figure 4 Fracture origin in a keatite specimen ground parallel with the tensile axis. (a) Low magnification photograph of the fracture origin area showing the fracture mirror and the concentrically located failure initiating flaw (arrowed). (b) Higher magnification photograph of the failure initiating flaw. Note its nearly semi-circular peripheral shape and its curvature (i.e. half a clam shell-like shape), and the second boundary near the arrow tip which is approximately concentric with the inner boundary, i.e. with the terminius of the highly curved section of the flaw. This flaw segment between the inner and the outer boundary, which is nearly in the plane of fracture, may represent the limited extent of slow crack growth expected in this material because of its high resistance to stress corrosion. Fracture stress 231 MPa.

agree well with those measured by fracture mechanics techniques in samples from the same body provided that the flaw sizes were sufficiently large in comparison with the grain size [9]. This corroborates the applicability of fracture mechanics to fine-grain materials. For flaw sizes smaller in comparison to the microstructure, internal stress effects from the thermal expansion anisotropy become important [9].

It is worthwhile to briefly illustrate some of the variations in machining flaws that occur in fine-grain materials, i.e. those materials where flaw boundaries are particularly clear so that these variations can be clearly seen. The variations are illustrated in the same body (Keatite crystallized glass) in order to compare changes in the same materials. Flaws forming perpendicular to the grinding direction are not necessarily flat, but often have a distinct curvature, e.g. like half a clam shell (Fig. 4). While the general difference in flaw shape is maintained over a number of samples (see Table II), there are variations, e.g. some more elongated flaws forming perpendicular to the grinding direction (Fig. 6). Also, there are variations in the angle of the flaws relative to the grinding direction and the fracture surface (Figs 7 and 8). Flaws often appear to develop in two or more stages as suggested by the changes in curvature that occur. This is more common for flaws perpendicular to the grinding direction (Fig. 9), but is also observed for flaws parallel with the grind direction (Fig. 6). Similar, but less pronounced, and flatter changes in flaw character, (e.g. Figs 4, 8) may represent such

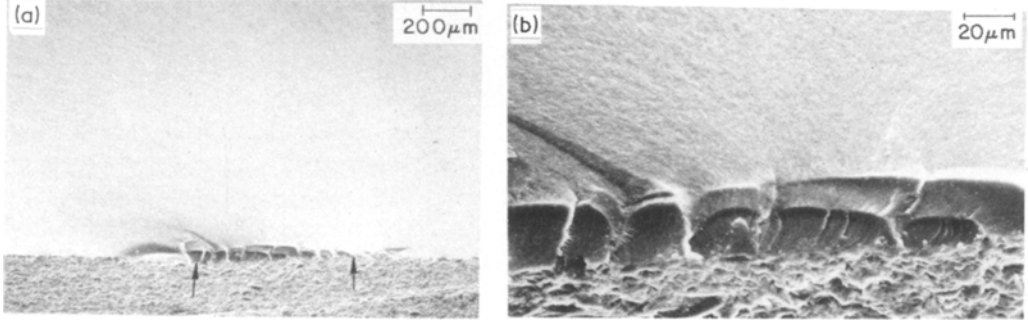

Figure 5 Fracture origin in a keatite specimen ground perpendicular with the tensile (bar) axis. (a) Lower magnification of the fracture origin area and (b) Higher magnification of part of the failure initiating flaw. Note the highly elongated character of the flaw and the fact that it consists of a series of shorter, substantially overlapping flaws. Note also the two sets of demarcations in the depth and changes in the non-planar character of the flaw indicating that it may have been generated in two stages. Fracture stress 99 MPa.

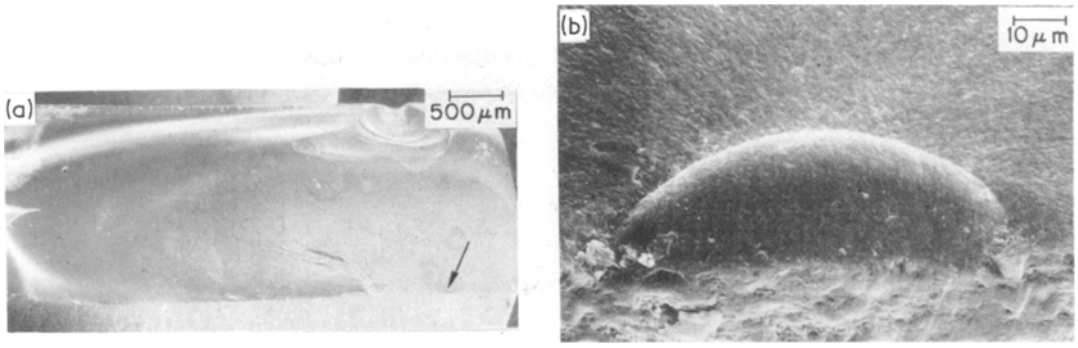

Figure 6 Example of an extremely elongated flaw at the origin of a keatite sample ground parallel with the tensile axis. (a) Low magnification photograph showing the entire fracture surface. Note the fracture mirror and the concentric fracture origin (arrowed). (b) Higher magnification photograph of the fracture origin. Note the substantially more elongated character of the flaw, which is extreme for a specimen ground parallel with the tensile axis, and that the flaw also has substantial curvature. Fracture stress 116 MPa.

multiple stages of development, but are felt to more likely represent slow crack growth prior to failure, since they also appear to represent a change from trans- to inter-granular failure, for example, similar to recent observations in MgF_2 [12]. Finally note that while flaws forming parallel with the grinding directions can be a fairly smooth, continuous flaw (Fig. 8), they are more often a series of a few separate cracks of varying degrees of overlap (Fig. 7).

3.2.2. Larger grain polycrystalline bodies

Larger grain bodies also can exhibit strength anisotropy as a function of grinding direction. Where specific fracture initiating flaws can be defined [13], these agree quantitatively with the strength anisotropy (Table II). Fracture energies calculated from observed flaws, examples of which are shown elsewhere, indicate a transition from single crystal to polycrystalline fracture energies [13].

Results from other studies [1, 4, 6, 8, 13, 14] and from work conducted in this study reveal that flaw sizes remain approximately constant so that, as one goes to bodies containing larger grains, the machining flaws become comparable to, or less than, the size of the large grains. Although orientation of preferred fracture planes in grains can vary the angle of the flaws [4, 13], failure-causing flaws are generally formed in those grains which have easy fracture planes orientated either parallel with or perpendicular to the grinding direction, as expected from the single crystal results. Larger flaws, i.e. those causing failure are presumably introduced in such grains because of their favour-

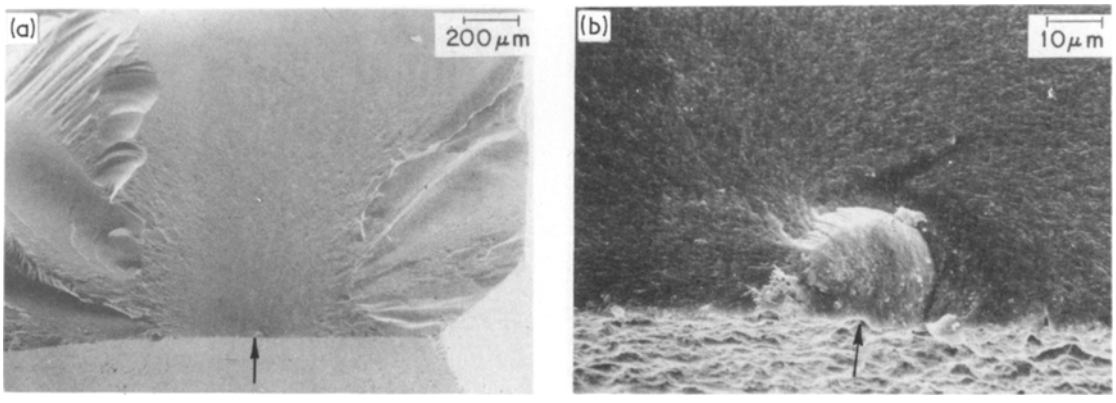

Figure 7 Example of a fracture initiating flaw whose plane is substantially different from that of the fracture surface in a keatite specimen ground parallel with a tensile axis. (a) Lower magnification photograph of much of the fracture surface. Note the clear fracture mirror and the approximately concentric fracture origin (arrowed). (b) Higher magnification photograph of the failure initiating flow. Note its curvature and very high angle relative to the fracture surface. Fracture stress 158 MPa.

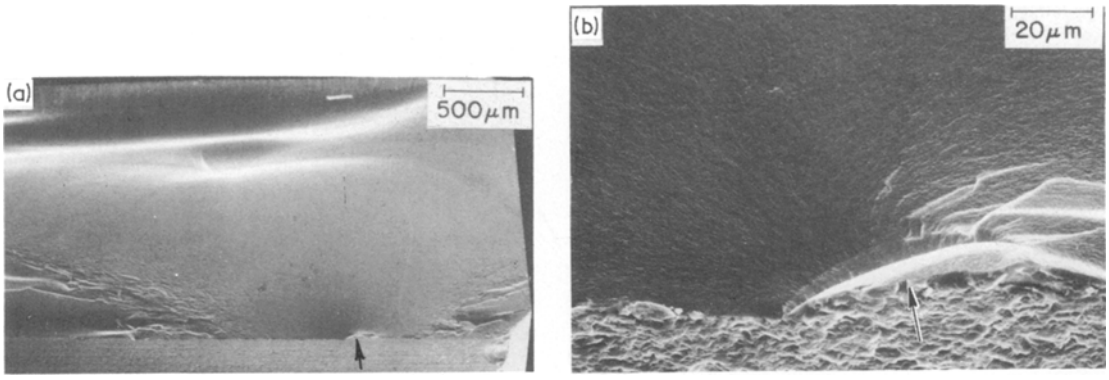

Figure 8 Example of flaw variation in a keatite specimen ground perpendicular to the tensile axis. (a) Low magnification photograph showing grinding striations on the tensile surface (approximately horizontal) and the fracture origin (arrowed) located inside the symmetric mirror. (b) Higher magnification photograph of the failure initiating flaw (arrowed) showing its substantially elongated character resulting from grinding perpendicular to the tensile axis. Note the angle of the flaw to the fracture surface and the first flaw boundary (nearest the tensile surface) terminating a fairly curved portion of the flaw and the second, deeper boundary outlining a lighter, flatter region very nearly in the plane of fracture. This latter region may well represent the limited amount of slow crack growth expected in this material similar to that indicated in Fig. 4. Failure stress 117 MPa.

able orientation for the introduction of such flaws. Such flaws in these grains are thus also favourably orientated for failure because of the relationship between the grinding direction and tensile axis in subsequent testing.

3.3. General discussion

General questions that must be addressed are what the flaw boundaries represent and whether they are significantly effected by stress corrosion or residual stresses. The observed flaw boundaries are generally felt to represent the original machining flaws. The stresses that cause flaw formation are not duplicated by the applied stress causing failure. Thus, since flaws prefer to propagate normal to the principal tensile stress, the flaw forms on one surface and propagates on another so that the interface between the two surfaces marks the original flaw. Although some cases of multiple interfaces, e.g. Figs 4 and 8 (see also Fig 4 of [13]), may in fact represent sub-critical crack growth, such as that due to environmental effects,

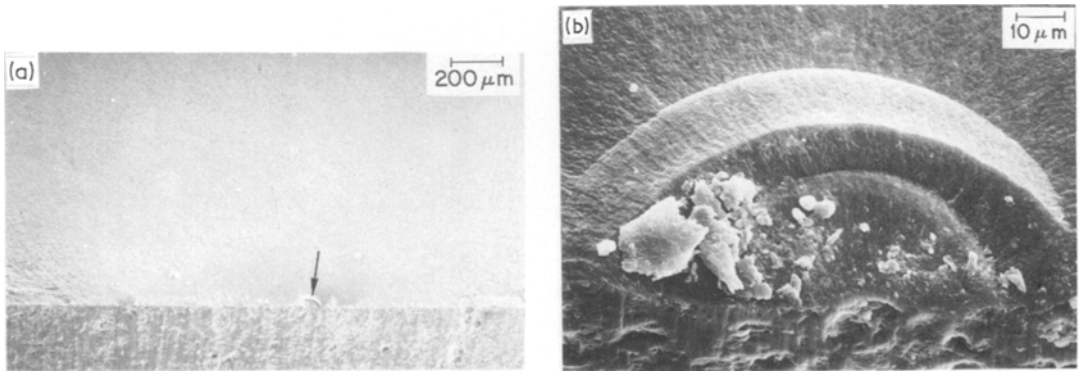

Figure 9 Failure initiating flaw in a keatite specimen ground parallel with the tensile axis indicating multiple stages of flaw development. (a) Lower magnification photograph of part of the fracture surface showing the fracture mist near the right and left hand portions of the photograph with the flaw approximately centred between the arrows. (b) Higher magnification photograph of the flaw. Note the three distinct sections of different flaw curvature, all of which are distinctly non-planar with the fracture surface. Such distinct sections are felt to represent different stages of flaw generation during machining, e.g. to represent vibration or changing stress levels during the flaw generation process. Note the contrast of the high curvature and low coincidence with fracture plane of these sections of the flaw in contrast to those in Figs 4 and 7 where additional flaw boundaries are attributed to slow crack growth. Fracture stress 103 MPa.

the present observations do not appear generally to account for such growth, i.e. such changes have not been clearly identified on most of the other materials. However, such growth, even if totally neglected, would not alter the present relative results unless it was very significantly different for the two sets of flaws. There is no reason to expect this, and the good correlation between observed strength ratios and those calculated from flaw geometry, for flaws large in comparison to the microstructure, indicates that flaw growth is not significantly different for the two sets of flaws. Important differences between measured and calculated fracture energies, when flaws are not sufficiently large in comparison to the grain size, are explained by other effects [9, 13] consistent with limited slow crack-growth.

Residual stresses from machining may also occur. Again, the good quantitative correlation of observed and calculated strength anistropy shows that any such stresses must be similar for the two sets of flaws; the fracture energy observations reported above support this. Thus, the absolute effect of such stresses is limited, e.g. is probably only significant as a source of scatter in the results.

In general, the single crystal and polycrystalline results in this work are similar to one another and are also comparable with results from earlier studies in glasses [2]. Thus, typically, two sets of flaws were formed during machining. One set, which is generally more elongated and often deeper, commonly forms parallel with the motion of the abrasive particle. The second set, more closely approaches a semi-circular shape, typically forms approximately perpendicular to the direction of motion of the abrasive particle. Such semi-circular shaped flaws may often not be planar, but have some curvature, e.g. they may have a shape approaching that of half a clam-shell.

Two modifications often arise in single crystals and in large grain bodies where there is one or more significantly preferred cleavage plane or fracture surface of failure. First, such preferred fracture tends to reduce the above noted curvature of flaws forming approximately perpendicular to the machining direction. Secondly, and more importantly, such preferred cleavage or fracture surfaces can alter the angular orientation of flaws relative to the machining direction by providing preferred planes or surfaces for flaw initiation. Thus flaws that would normally form parallel with or perpendicular to the machining direction, except for statistical variations, may form on preferred fracture planes having angles other than $\pm 0^\circ$ or $\pm 90^\circ$ to the machining direction.

Results of this paper reinforce previous observations [8, 14] that, within a given material, the flaw size does not change greatly over a wide range of grain sizes including single crystals, as can be seen by comparing the results of this study with those of other studies [4, 7, 8, 13, 14]. In fact, despite specimens being machined over a period of several years by a variety of operators with various degrees of wheel dressing, different grinding wheels, and some variation in feed rate, flaw sizes within a given material ranging from single crystals to very fine grain, polycrystalline bodies vary on average by a factor of only about 2, e.g. compare the single crystal results of Table II with polycrystalline $MgAl_2O_4$ results [4, 7, 14]. This must be a major factor in the common agreement of strength–microstructure data collected by a wide variety of investigators for a given material [7, 16].

Two points arise from the almost constant flaw size which is nearly, or fully, independent of grain size. Firstly, this has important implications for strength–grain size models and fracture energies for use in fracture mechanics predictions, including life predictions, all of which are discussed elsewhere [7, 9, 13, 15]. Secondly, the anisotropy in strength as a function of the grinding directions relative to the tensile axis may diminish, or even disappear, as the flaw size (C) approaches the grain size (G). Consider the more elongated flaws forming nearly parallel to the machining direction and a series of bodies of different average grain sizes. As the grain size decreases so the typical flaw would extend over 2 to 4 grains; only part of the flaw may form due to unfavourable orientations of preferred fracture planes or grain boundaries of grains along the flaws path of formation. Alternatively, if the flaw forms completely, portions of the flaw may be at substantially lower angles relative to the tensile axis and hence may make the flaw less effective. Thus, such strength anisotropy may be similar at the extremes of grain size, i.e. fine grain bodies and single crystals, but less at intermediate grain sizes where $C \approx G$. Such effects may, however, be difficult to accurately determine because of typical grain size variations in any given body.

4. Summary and conclusions

Grinding introduces two basic sets of flaws, one set typically forms at an angle of $\sim 0^\circ$ to the grinding direction, i.e. abrasive motion direction, and the other forms at an angle of $\sim 90^\circ$ to the grinding direction. In single crystals there can be systematic shifts from these angles due to the orientation of preferred fracture planes or surfaces relative to the grinding direction. There can also be variations of the orientations of the flaw sets in polycrystalline bodies. In larger grain bodies these variations can occur due to the orientation of preferred fracture planes or surfaces in the grains. In any polycrystalline body, statistical variations of local grinding forces or in the material may also cause some variation of flaw angles. However, generally, the differences in geometry between the two sets of flaws is an important, and generally dominant, factor in the anisotropy of strength that results from testing specimens ground parallel with the tensile axis against specimens ground perpendicular to the tensile axis.

Acknowledgements

Mr Newell, Mr Bender and Mrs. Morey are thanked for their excellent scanning electron microscopy to determine and photograph fracture origins. Keatite samples were provided by Dr J. Ritter, University of Massachusetts.

References

1. R. W. RICE, in "The Science of Ceramic Machining and Surface Finishing", NBS Special Pub. 348, 365–376, edited by S. J. Schneider and R. W. Rice (Government Printing Office, Washington, D.C. 20402, 1972).
2. J. J. MECHOLSKY, S. W. FREIMAN and R. W. RICE, *J. Amer. Ceram. Soc.* **60** (1977) 114.
3. P. F. BECHER, *ibid.* **56** (1976) 59.
4. R. W. RICE and J. J. MECHOLSKY, Jr, Proceedings of the Conference on Science of Ceramic Machining and Surface Finishing, II, edited by B. J. Hockey and R. W. Rice, National Bureau of Standards, Special Publication 562 (National Bureau of Standards, Washington, D.C., 1979) pp. 351–378.
5. J. J. MECHOLSKY, S. W. FREIMAN and R. W. RICE, *J. Mater. Sci.* **11** (1976) 1310.
6. R. W. RICE, in "Surfaces and Interfaces of Glass and Ceramics", edited by V. D. Frechett, W. C. LaCourse and V. L. Burdick (Plenum Press, New York, 1974) pp. 439–472.
7. *Idem*, Proceedings of the Conference on Science of Ceramic Machining and Surface Finishing, II, edited by B. J. Hockey and R. W. Rice, National Bureau of Standards, Special Publication 562 (National Bureau of Standards, Washington, D.C., 1979) pp. 429–454.
8. *Idem*, Proceedings of the Conference on Processing of Crystalline Materials, edited by H. Palmour III, R. F. Davis and T. M. Hare, (Plenum Press, New York, 1978) pp. 303–319.
9. R. W. RICE, R. C. POHANKA and W. J. MCDONOUGH, *J. Amer. Ceram. Soc.* **63** (1980) 703.
10. G. K. BANSAL, W. H. DUCKWORTH and D. E. NIESZ, *ibid.* **55** (1976) 289.
11. *Idem, ibid.* **59** (1976) 472.
12. J. J. MECHOLSKY, unpublished work.
13. R. W. RICE, S. W. FREIMAN and J. J. MECHOLSKY, Jr, *J. Amer. Ceram Soc.* **63** (1980) 129.
14. *Idem*, Proceedings of the Second Army Materials Technology Conference, edited by J. J. Burke, A. E. Gorum and R. N. Katz (Brook Hill Publishing Co., Chestnut Hill, Massachusetts, 1974) pp. 287–343.
15. R. W. RICE, S. W. FREIMAN, R. C. POHANK, J. J. MECHOLSKY, Jr and C. Cm. WU, in "Fracture Mechanics of Ceramics", Vol. 4, edited by R. C. Bradt, D. P. H. Hasselman and F. F. Lange, (Plenum Press, New York, 1978) pp. 849–876.
16. R. W. RICE, *Proc. British Ceram. Soc.* **20** (1972) 205.

Received 15 May and accepted 2 September 1980.